$^1S_0$ Nucleon-Nucleon Phase Shift with Effective Field Theory
Report for Project #2

Hao Lin, Han Liu, Dillon Frame

December 12, 2017

Abstract

In this report, we describe the extension of our code from project #1 to more realistic, chirally motivated NN-potentials. For various orders, we compute the $^1S_0$ phase shifts after fitting the low energy coefficients (LECs) to the Nijmegen phase shift data. We also present estimates of the breakdown scale of this theory, and the cutoff dependence of the phase shifts.

1 Introduction

In this project, we wish to extend our previous work on the solution of the Lippmann-Schiwinger Equation for a phenomenological potential to using a more realistic potential motivated by Pionless Effective Field Theory.

In the first section, we provide some motivation of this theory, and describe the form of the nucleon-nucleon interaction. Then we simplify this interaction to only include the spin-independent and isospin-independent parts, so that we can once again focus on the $^1S_0$ phase shift. We also discuss how to extend this description of the interaction by including one-pion exchange terms (OPE) by using the Yukawa potentials from Project #1.

In the second section, we detail the implementation of the potential, at leading order (LO), next-to-leading order (NLO), and next-to-next-to-leading order (NNLO) in this potential. We detail our fitting process for determining the low energy coefficients for each potential.

Finally, we provide the calculated phase shifts at each order, the values we obtained for the low energy coefficients, as well as several Lapage plots showing the improvement in the errors as we go to higher orders.

2 Pionless EFT

Pionless Effective Field Theory is a lower energy version of Chiral EFT where the pion degree of freedom is removed, and we are left with only contact interactions between the nucleons. These interactions take the form:

$$V^{LO}\left(\vec{q}, \vec{k}\right) = C_S + C_T \vec{\sigma_1} \cdot \vec{\sigma_2}$$

$$V^{NLO}\left(\vec{q}, \vec{k}\right) = C_1 \vec{q}^2 + C_2 \vec{k}^2 + \vec{\sigma_1} \cdot \vec{\sigma_2}\left(C_3 \vec{q}^2 + C_4 \vec{k}^2\right)$$
$$+ iC_5 \frac{\vec{\sigma_1} + \vec{\sigma_2}}{2} \cdot \vec{q} \times \vec{k} + C_6 \vec{q} \cdot \vec{\sigma_1} \vec{q} \cdot \vec{\sigma_2}$$
$$+ C_7 \vec{k} \cdot \vec{\sigma_1} \vec{k} \cdot \vec{\sigma_2}$$

where $\vec{q} = \vec{p} - \vec{p'}$ is the momentum transfer, and $\vec{k} = \frac{\vec{p} + \vec{p'}}{2}$ is the average momentum, and $\vec{p}, \vec{p'}$ are the relative momenta.

Since we are interested in a spin-independent interaction, we can drop all the terms involving the Pauli matricies. We then have the simplified potentials:

$$V^{LO}_{^1S_0}(p, p') = C_0 \tag{1}$$

$$V^{NLO}_{^1S_0}(p, p') = C_2\left(p^2 + p'^2\right) \tag{2}$$

$$V^{NNLO}_{^1S_0}(p, p') = C_4\left(p^4 + p'^4\right) + C'_4 p^2 p'^2 \tag{3}$$

Since we are solving the Lippmann-Schwinger equation using a discretized mesh, it is necessary to change the form of our potential regulator to handle the high momentum / short range points. These regulators are functions of some cutoff Λ, and are applied to the potential via the transformation

$$V(p, p') \to f_\Lambda(p) V(p, p') f_\Lambda(p) \tag{4}$$

$$C_i = C_i - \epsilon \frac{f(\vec{C})}{(\nabla f)^2} \frac{\partial f}{\partial C_i},$$

$$\epsilon \sim 0.01$$

As opposed to our hard cutoff from the previous project:

$$f_\Lambda(p) = \theta\left(\Lambda - p\right) \tag{5}$$

we now wish to use a regulator of the form

$$f_\Lambda(p) = \exp\left[-p^4/\Lambda^4\right] \tag{6}$$

This will cause the contact terms to be more well-behaved, and we can study the behaviour of the phase shifts as a function of this cutoff.

3   Methods & Implementation

Since we have started with the code from Project #1 s our baseline, there were not many modifications that needed to be made. We adjusted the form of the potential to include the four terms in Eqns. [1-3], as well as including the regulator in Eqn. [5].

from the pheonomenological potential in project 1 for E_{cm} between 0.05 and 5 MeV

For each order, we performed a fit to the phase shifts ~~from the Nijmegen NN-online database for lab energies between 0.1 and 2 MeV~~. The fit was performed using a simple Gradient Descent method using a five-point stencil to approximate the derivative at each point.

The function we were minimizing was the sum of the squares of the residuals between the computed values and real values for the phase shifts.

Gradient decent works by starting at a point in the parameter space, and computing the gradient of the function at that point. This gradient points along the steepest descent of the function towards the minimum. By moving a small amount along the gradient, we can eventually arrive at the minimum of the function.

To approximate the derivative at a particular point, for one particular coupling, we compute the five-point stencil

$$\frac{df(x)}{dx} \approx \frac{1}{12h}[f(x+2h) + 8f(x+h)$$
$$- 8f(x-h) + f(x-2h)]$$

where h is a small parameter. So our methods goes something like:

- Initialize the appropriate couplings C_0, C_2, etc. for the order being simulated.

- For each coupling C_i, compute the gradient df/dC_i

- After the gradients are computed, make an adjustment to each coupling by an amount proportional to the gradient ~~$C_i = C_i + \epsilon(df/dC_i)$~~.

- Repeat this process until the results are converged

4   Results

We now present the results for the $^1S_0$ phase shifts calculated at LO,NLO, and NNLO. In Fig. 1, we show the calculated phase shifts as a function of center-of-mass energy for each order, compared to the phenomenological results from Project #1.
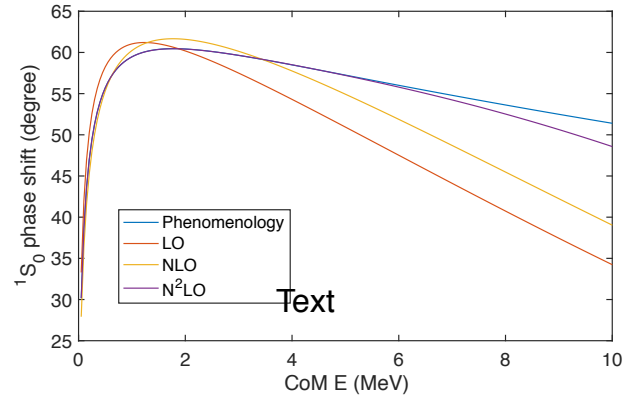

Figure 1: $^1S_0$ phase shifts calculated at LO,NLO, and NNLO. Phenomenological results also shown.

Tabulated below are the values for the low energy coefficients we obtained at each order.

Coefficient	LO	NLO	NNLO
C_0 (MeV * fm^3)	-106.572	-92.5367	-99.8683
C_2 (MeV * fm^5)	-	-52.1465	92.4564
C_4 (MeV * fm^7)	-	-	-342.975
C_4' (MeV * fm^7)	-	-	-426.396

Table 1: LECs for LO,NLO, and NNLO simultions.

If we look at the errors of each order, we arrive at the plot in Fig. 2. Notice for low energy, the errors at each order improve dramatically, but as we approach 10 MeV, we stop seeing improvement by including higher order terms.

In Fig. 3, we show the cutoff dependence of the NLO phase shifts. We varied Λ in the range $0.75m_\pi$ to $3m_\pi$, and computed the errors in the phase shift in each case. Note also that the LECs are 'running', as \Lambda varies.

In Fig. 4, we modified the potential at each order to include the longest range, one-pion exchange po-

2

tential, which we used in Project #1. We note that the agreement is much better across the board.

Tabulated below are the new values of the LECs

\Lambda ~ 1.4 m_{\pi}

Coefficient	LO	NLO	NNLO
C_0 (MeV * fm^3)	-58.2011	-57.9153	-56.0252
C_2 (MeV * fm^5)	-	-0.638217	18.2039
C_4 (MeV * fm^7)	-	-	-43.0476
C_4' (MeV * fm^7)	-	-	-22.465

Table 2: LECs for LO,NLO, and NNLO with a OPEP.

If we now look at the errors in these updated phase shifts, we can see that the breakdown scale is now ~~on the order of 100 MeV~~, as compared to the 10 MeV we got from not including the pion.
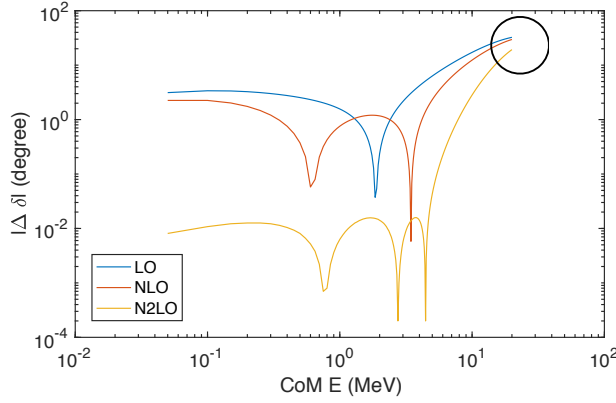
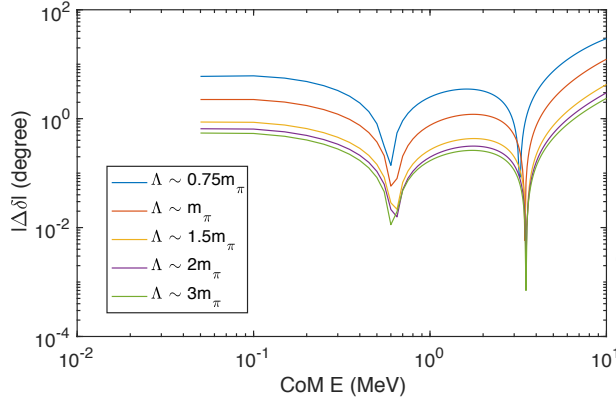Figure 2: Errors in the phase shifts at each order.

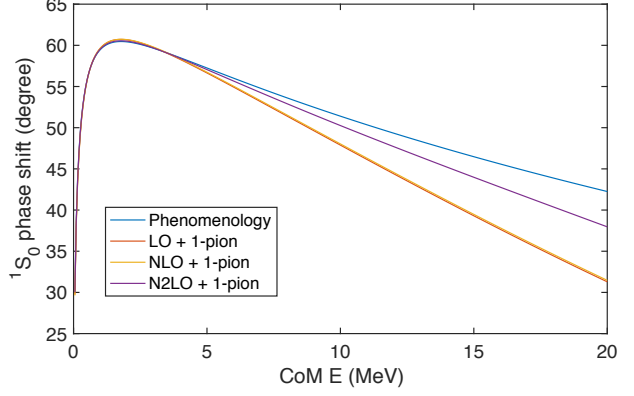Figure 3: Cutoff dependence of the NLO phase shifts.

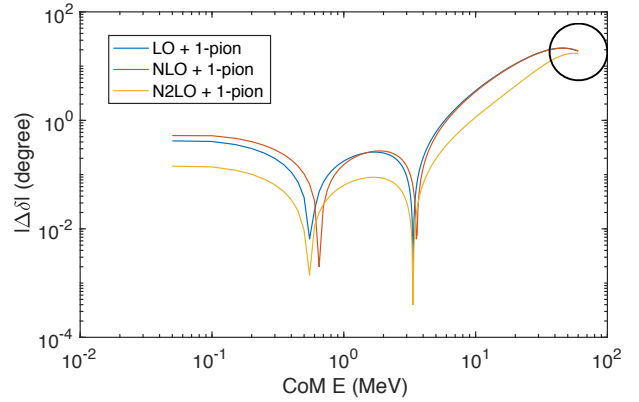Figure 4: Phase shifts calculated by including a simple OPE potential

Figure 5: Error in the phase shits for varying orders.

Errors get smaller as \Lambda gets larger. Once the cutoff \Lambda goes beyond the breakdown scale, the improvemnets brought about by larger cutoffs become negligible.

1. S. Bogner and M. Hjorth-Jensen, *Project 1 Assignment Notes*, `https://manybodyphysics.github.io/NuclearForces/doc/web/course.html`

2. S. Bogner and M. Hjorth-Jensen, *Project 2 Assignment Notes*, `https://manybodyphysics.github.io/NuclearForces/doc/Projects/2017/Project2/pdf/Project2.pdf`